

## Supporting Materials

### Decorating Pt@cyclodextrin nanoclusters on C<sub>3</sub>N<sub>4</sub>/MXene for boosting the photocatalytic H<sub>2</sub>O<sub>2</sub> production

Haiguang Zhu,<sup>§</sup> Qiang Xue,<sup>§</sup> Guangyan Zhu, Yong Liu, Xinyue Dou, and Xun Yuan\*

College of Materials Science and Engineering, Qingdao University of Science and Technology (QUST), 53 Zhengzhou Rd., Shibei District, Qingdao 266042, P. R. China

Email address: [yuanxun@qust.edu.cn](mailto:yuanxun@qust.edu.cn)

<sup>§</sup>These authors contributed equally to this paper.



**Figure S1.** Digital photographs of the CS380 electrochemical workstation (a) and the three-electrode cell (b).

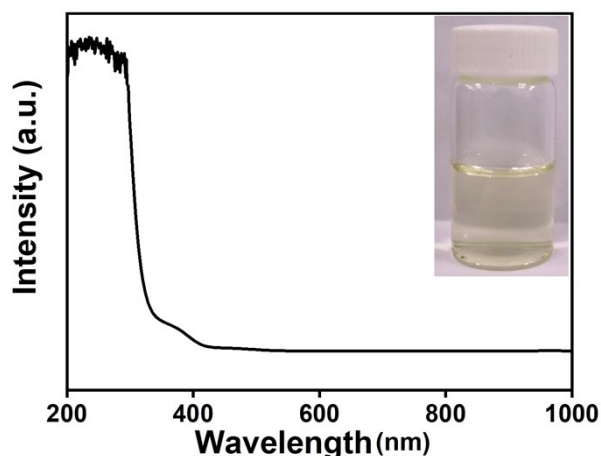


**Figure S2.** UV-vis absorption spectrum of the Pt(II)-β-CD complexes and the image of the corresponding sample solution (inset).

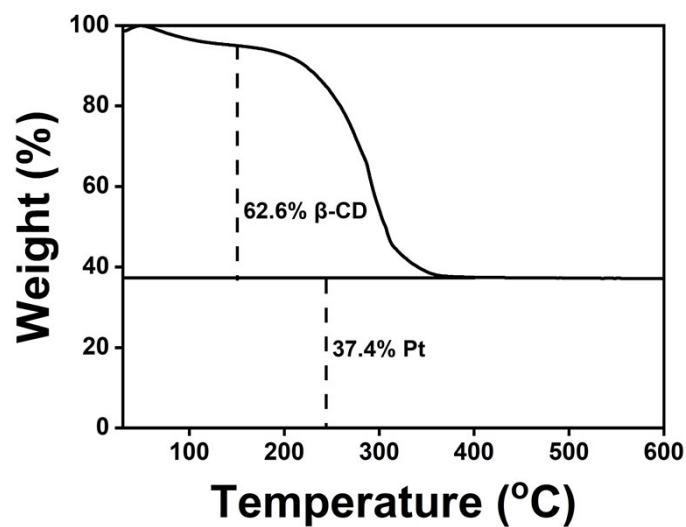


**Figure S3.** The TGA curve of Pt@ $\beta$ -CD NCs.

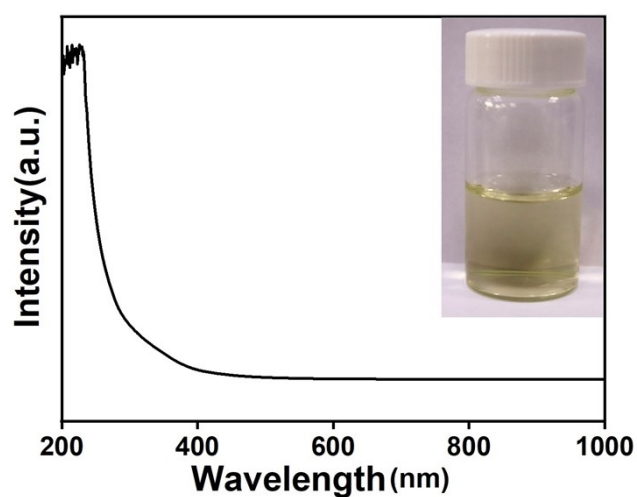


**Figure S4.** UV-vis absorption spectrum of the Pt(II)- $\beta$ -CD complexes after NaBH<sub>4</sub>-reduction and the image of the corresponding sample solution (inset).

**Note:** The optical absorption spectrum and solution color are similar to that of Pt(II)- $\beta$ -CD complexes before NaBH<sub>4</sub>-reduction (Figure S2), indicating unsuccessful formation of Pt NCs@ $\beta$ -CD using NaBH<sub>4</sub> as reducing agent.

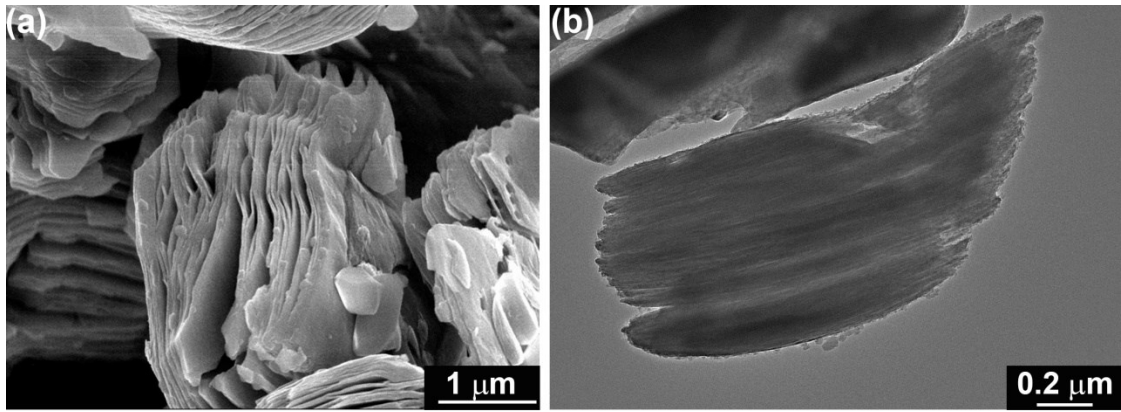


**Figure S5.** SEM image (a) and TEM image (b) of the as-prepared MXene ( $\text{Ti}_2\text{C}_3$ ).

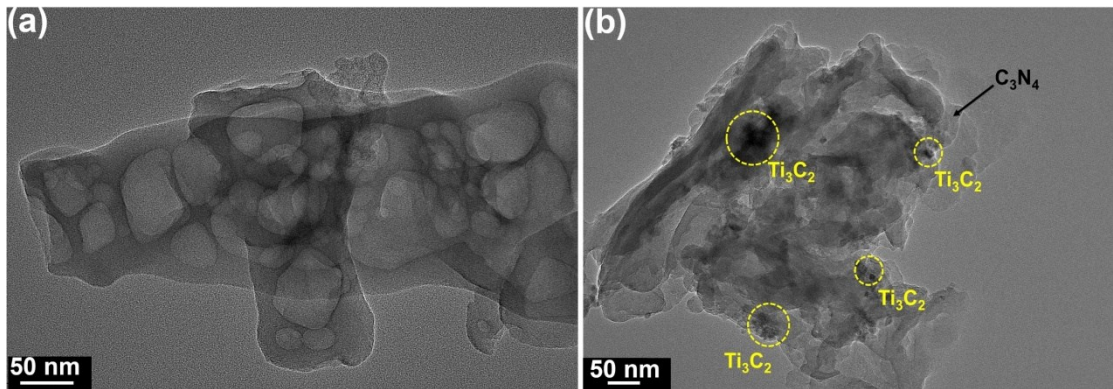


**Figure S6.** TEM images of  $\text{C}_3\text{N}_4$  before (a) and after (b) deposition of MXene ( $\text{Ti}_3\text{C}_2$ ).

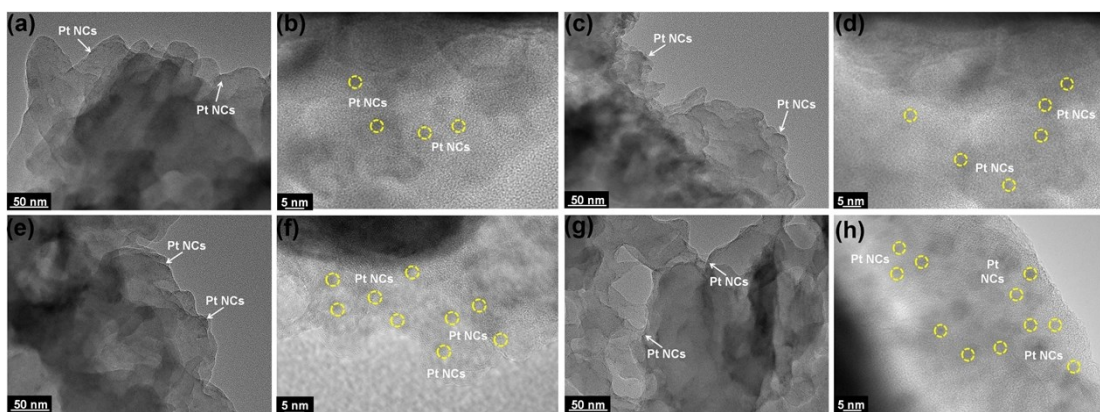


**Figure S7.** TEM and corresponding HRTEM images of Pt@ $\beta$ -CD/ $\text{C}_3\text{N}_4$ -1 (a-b), Pt@ $\beta$ -CD/ $\text{C}_3\text{N}_4$ -2 (c-d), Pt@ $\beta$ -CD/ $\text{C}_3\text{N}_4$ -3 (e-f), and Pt@ $\beta$ -CD/ $\text{C}_3\text{N}_4$ -5 (g-h). Note: the HRTEM image of Pt@ $\beta$ -CD/ $\text{C}_3\text{N}_4$ -4 is displayed in the inset of Figure 2b.

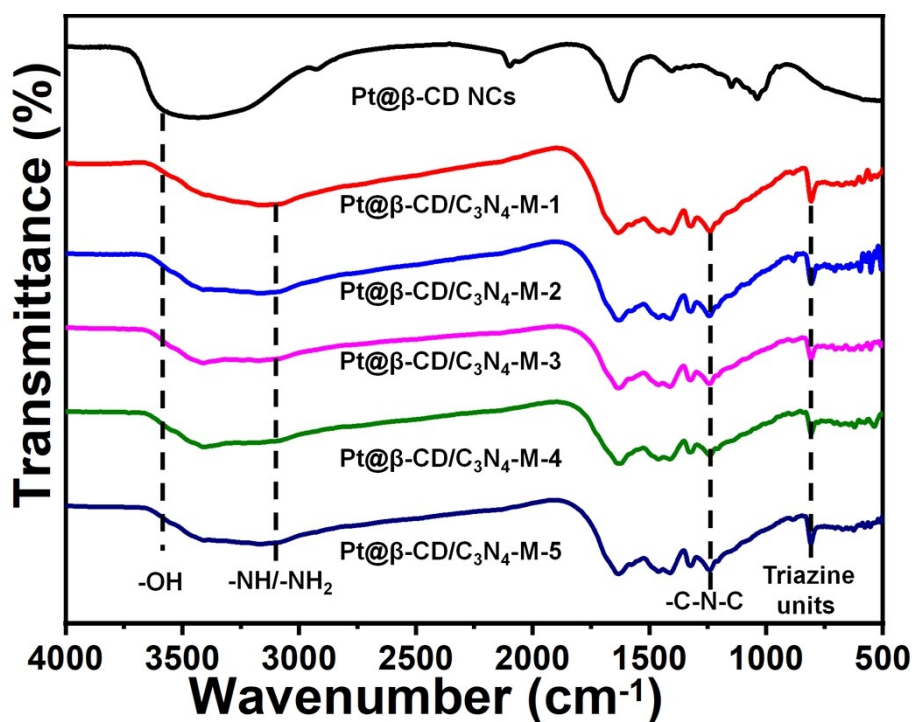


**Figure S8.** FTIR spectra of the pristine Pt@β-CD NCs and five Pt@β-CD/C<sub>3</sub>N<sub>4</sub>-M samples with the loading of 1-5 wt.% Pt species.

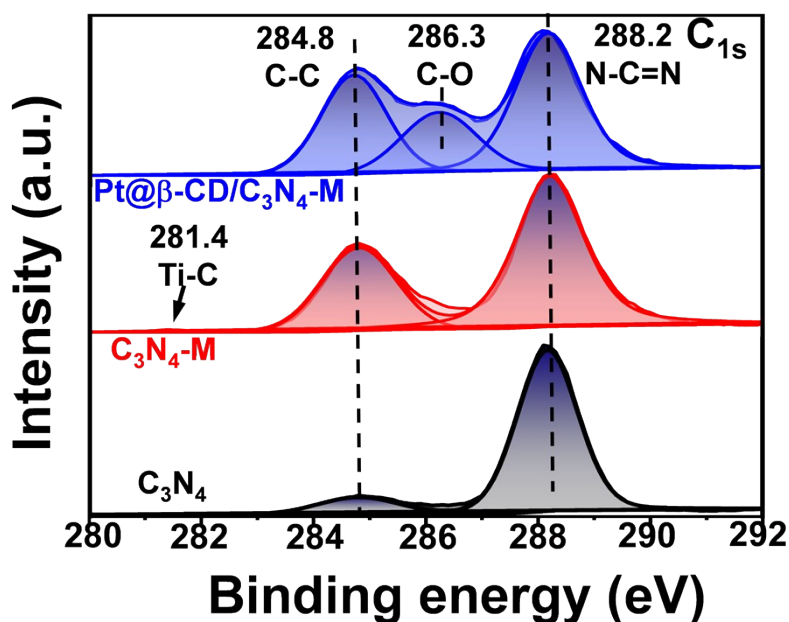


**Figure S9.** XPS survey of C 1s of the pristine C<sub>3</sub>N<sub>4</sub>, C<sub>3</sub>N<sub>4</sub>-M, and Pt@β-CD/C<sub>3</sub>N<sub>4</sub>-M photocatalyst.

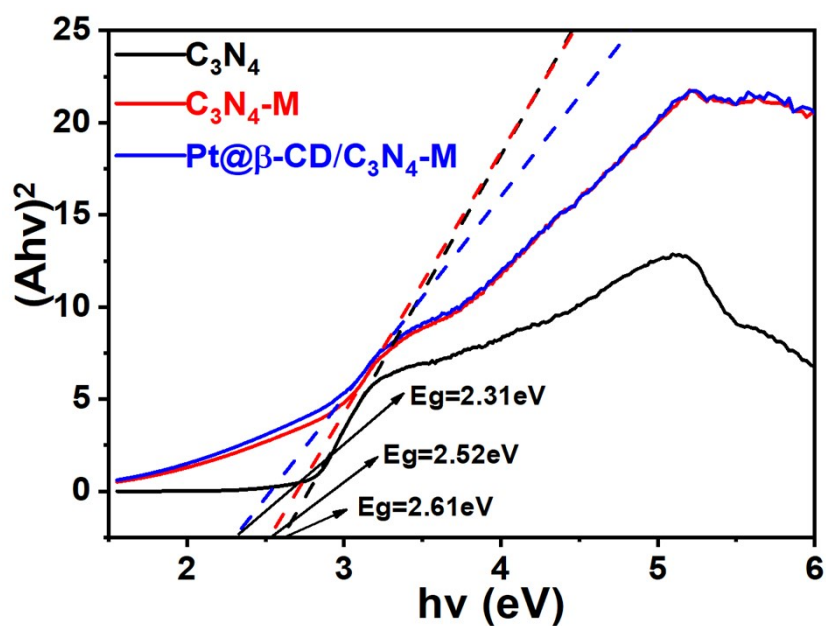


**Figure S10.** The calculated energy gap ( $E_g$ ) of the pristine  $C_3N_4$ ,  $C_3N_4-M$ , and  $Pt@β-CD/C_3N_4-M$  photocatalyst according to their corresponding UV-Vis DRS absorption spectra.

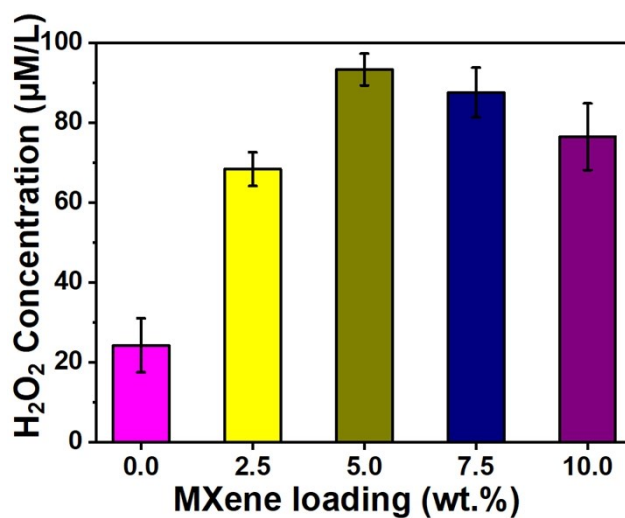


**Figure S11.** The MXene loading influence of  $C_3N_4-M$  on the photocatalytic  $H_2O_2$  production within 60 min.



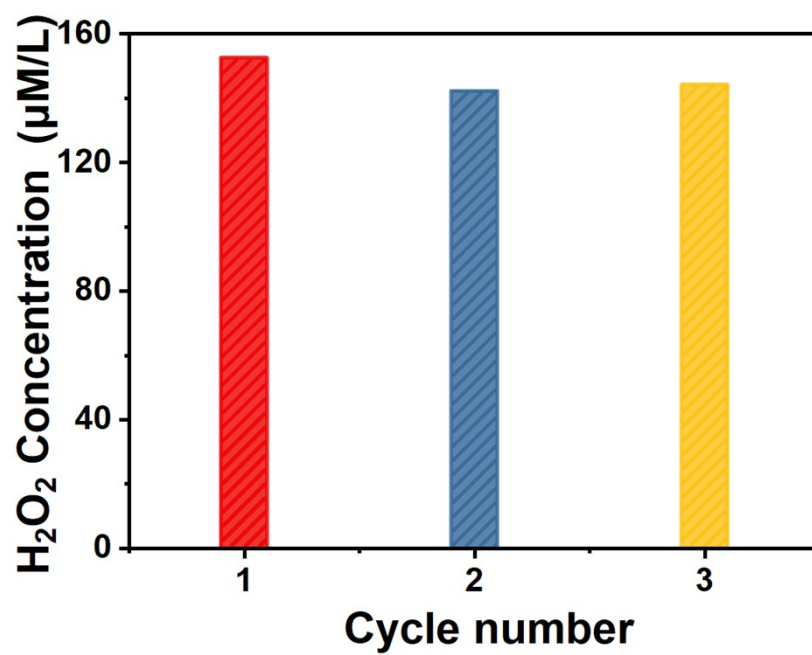


**Figure S12.** Durability test of the Pt@ $\beta$ -CD/C<sub>3</sub>N<sub>4</sub>-M in photocatalytic H<sub>2</sub>O<sub>2</sub> production.

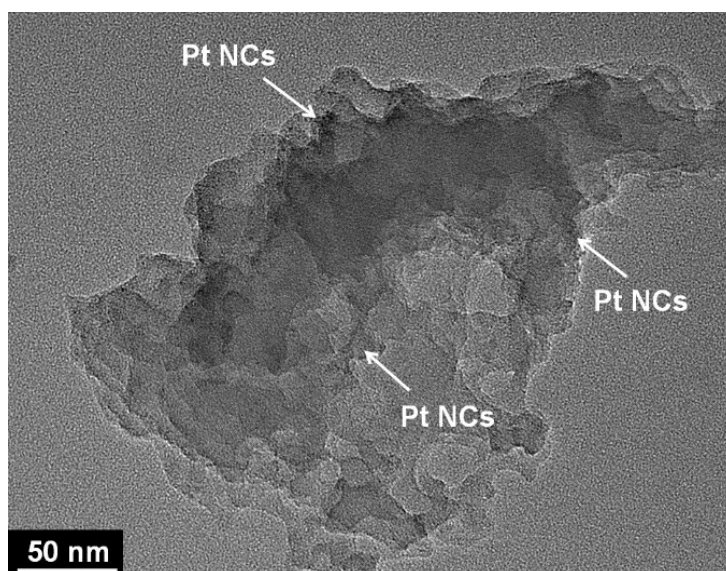


**Figure S13.** TEM image of the Pt@ $\beta$ -CD/C<sub>3</sub>N<sub>4</sub>-M after photocatalytic test.

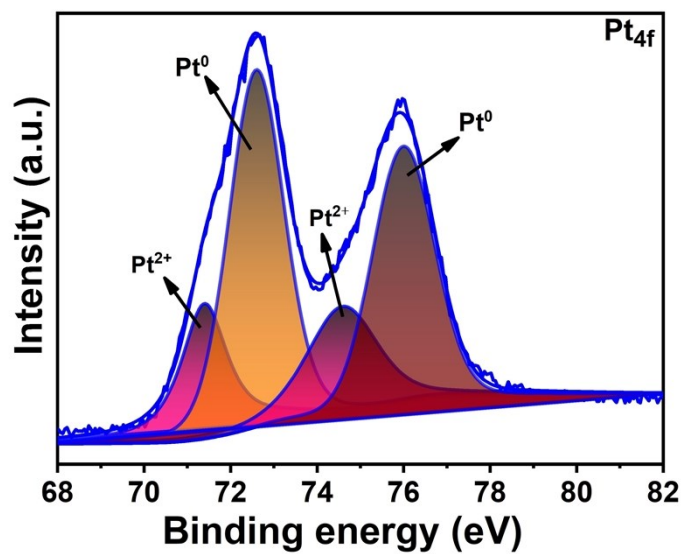


**Figure S14.** XPS survey of Pt 4f species in the Pt@ $\beta$ -CD/C<sub>3</sub>N<sub>4</sub>-M after photocatalytic test.

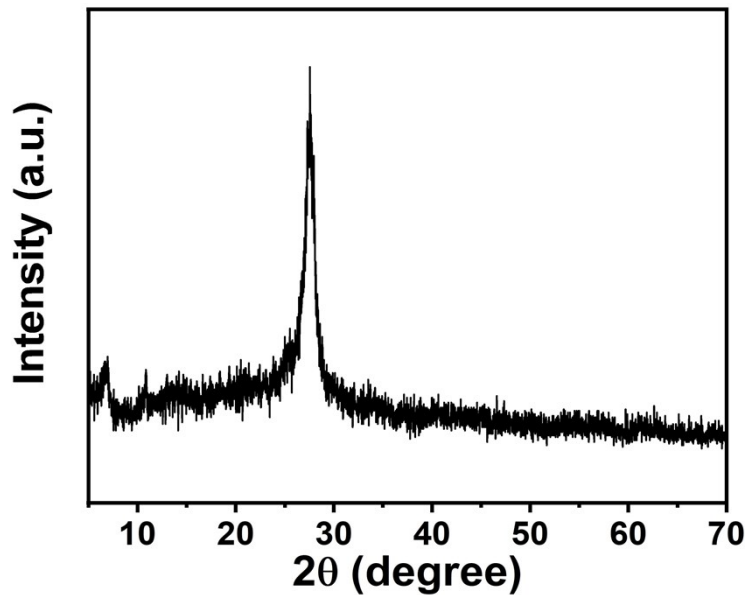


**Figure S15.** XRD pattern of the Pt@ $\beta$ -CD/C<sub>3</sub>N<sub>4</sub>-M after photocatalytic test.

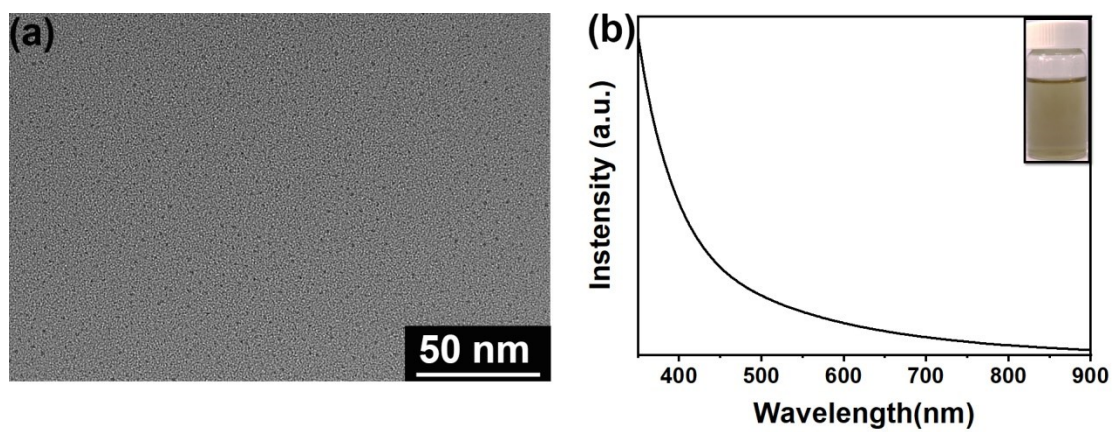


**Figure S16.** TEM image (a) and UV-Vis absorption spectrum of Pt@GSH NCs and the photo of corresponding NC solution taken under visible light



**Table S1.** Comparison of the photocatalytic performance of the Pt@ $\beta$ -CD/C<sub>3</sub>N<sub>4</sub>-M with other C<sub>3</sub>N<sub>4</sub>-based photocatalysts reported in the literature.

Photocatalyst	Dosage (g·L <sup>-1</sup> )	Light wavelength	Reaction solution	Yield (μM·g <sup>-1</sup> ·h <sup>-1</sup> )	Ref.
g-C <sub>3</sub> N <sub>4</sub> /BDI	1.67	λ > 420 nm,	Water	17.05	1
g-C <sub>3</sub> N <sub>4</sub> /PDI	1.67	λ > 420 nm	Water	21.04	2
g-C <sub>3</sub> N <sub>4</sub> /PDI/rGO	1.67	λ > 420 nm,	Water	24.17	3
3DOM-g-C <sub>3</sub> N <sub>4</sub> -PW <sub>11</sub>	1	λ > 320 nm	Water	35.00	4
MMO@C <sub>3</sub> N <sub>4</sub>	1	Solar light	Water, pH =3	40.00	5
Ag@U-g-C <sub>3</sub> N <sub>4</sub> -NS	1	λ > 420 nm,	Water, pH =3	≈69.00	6
Cv-g-C <sub>3</sub> N <sub>4</sub>	1	λ > 420 nm	Water	≈90.00	7
PI-NCN	1	λ > 420 nm	Water	≈92.00	8
DCN	0.83	λ > 420 nm	20 vol % IPA/water	96.80	9
Bi <sub>4</sub> O <sub>5</sub> Br <sub>2</sub> /g-C <sub>3</sub> N <sub>4</sub>	1	λ > 420 nm	Water	124.00	10
TC/pCN	1	λ > 420 nm	10 vol% IPA/water	131.71	11
R <sub>370</sub> -C <sub>3</sub> N <sub>4</sub>	1	λ > 420 nm	Water	170.00	12
Mesoporous g-C <sub>3</sub> N <sub>4</sub>	4	λ > 420 nm	90 vol% EA/water	≈183.50	13
PEI/C <sub>3</sub> N <sub>4</sub>	1	Solar light	water	208.10	14
g-C <sub>3</sub> N <sub>4</sub> -CNTs	1	λ ≥ 400 nm	10 vol % FA/water	487.00	15
Pt@β-CD/C <sub>3</sub> N <sub>4</sub> -M	1	λ ≥ 400 nm	Water	147.10	<b>This work</b>

BDI: biphenyl diimide; PDI: pyromellitic diimide; rGO: reduced graphene oxide; 3DOM g-C<sub>3</sub>N<sub>4</sub>: three dimensionally ordered macroporous graphitic carbon nitride; PW<sub>11</sub>: polyoxometalate (POMs) cluster of [PW<sub>11</sub>O<sub>39</sub>]<sup>7-</sup>; MMO: Mixed-Metal Oxide; Ag@U-g-C<sub>3</sub>N<sub>4</sub>-NS: PI-NCN: Ag NPs decorated on ultrathin g-C<sub>3</sub>N<sub>4</sub> nanosheets; Cv-g-C<sub>3</sub>N<sub>4</sub>: Carbon vacancy contained g-C<sub>3</sub>N<sub>4</sub>; PI-NCN: perylene imides deposited on g-C<sub>3</sub>N<sub>4</sub> nanosheets; DCN, nitrogen defective g-C<sub>3</sub>N<sub>4</sub>; R<sub>370</sub>-C<sub>3</sub>N<sub>4</sub>: Reduced g-C<sub>3</sub>N<sub>4</sub> prepared at reduction temperature of 370 °C; TC/pCN: Ti<sub>3</sub>C<sub>2</sub>/porous g-C<sub>3</sub>N<sub>4</sub>; PEI: polyethylenimine; IPA: isopropanol; EA: ethanol; FA: formic acid.

## Reference

- 1 Y. Kofuji, S. Ohkita, Y. Shiraishi, H. Sakamoto, S. Tanaka, S. Ichikawa and T. Hirai, *ACS Catal.*, 2016, **6**, 7021-7029.
- 2 Y. Shiraishi, S. Kanazawa, Y. Kofuji, H. Sakamoto, S. Ichikawa, S. Tanaka and T. Hirai, *Angew. Chem. Int. Ed.*, 2014, **53**, 13454-13459.
- 3 Y. Kofuji, Y. Isobe, Y. Shiraishi, H. Sakamoto, S. Tanaka, S. Ichikawa and T. Hirai, *J. Am. Chem. Soc.*, 2016, **138**, 10019-10025.
- 4 S. Zhao, X. Zhao, H. Zhang, J. Li and Y. Zhu, *Nano Energy*, 2017, **35**, 405-414.
- 5 R. Wang, K. Pan, D. Han, J. Jiang, C. Xiang, Z. Huang, L. Zhang and X. Xiang, *ChemSusChem*, 2016, **9**, 2470-2479.
- 6 J. Cai, J. Huang, S. Wang, J. Iocozzia, Z. Sun, J. Sun, Y. Yang, Y. Lai and Z. Lin, *Adv. Mater.*, 2019, **31**, 1806314.
- 7 S. Li, G. Dong, R. Hailili, L. Yang, Y. Li, F. Wang, Y. Zeng and C. Wang, *Appl. Catal. B: Environ.*, 2016, **190**, 26-35.
- 8 L. Yang, G. Dong, D. L. Jacobs, Y. Wang, L. Zang and C. Wang, *J. Catal.*, 2017, **352**, 274-281.
- 9 L. Shi, L. Yang, W. Zhou, Y. Liu, L. Yin, X. Hai, H. Song and J. Ye, *Small*, 2018, **14**, 1703142.
- 10 X. Zhao, Y. You, S. Huang, Y. Wu, Y. Ma, G. Zhang and Z. Zhang, *Appl. Catal. B: Environ.*, 2020, **278**, 119251.
- 11 Y. Yang, Z. Zeng, G. Zeng, D. Huang, R. Xiao, C. Zhang, C. Zhou, W. Xiong, W. Wang, M. Cheng, W. Xue, H. Guo, X. Tang and D. He, *Appl. Catal. B: Environ.*, 2019, **258**, 117956.
- 12 Z. Zhu, H. Pan, M. Murugananthan, J. Gong and Y. Zhang, *Appl. Catal. B: Environ.*, 2018, **232**, 19-25.
- 13 Y. Shiraishi, Y. Kofuji, H. Sakamoto, S. Tanaka, S. Ichikawa and T. Hirai, *ACS Catal.*, 2015, **5**, 3058-3066.
- 14 X. Zeng, Y. Liu, Y. Kang, Q. Li, Y. Xia, Y. Zhu, H. Hou, M. H. Uddin, T. R. Gengenbach, D. Xia, C. Sun, D. T. McCarthy, A. Deletic, J. Yu and X. Zhang, *ACS Catal.*, 2020, **10**, 3697-3706.
- 15 S. Zhao, T. Guo, X. Li, T. Xu, B. Yang and X. Zhao, *Appl. Catal. B: Environ.*, 2018, **224**, 725-732.